ACS OMEGA

http://pubs.acs.org/journal/acsodf

Article

Localization of Noise in Biochemical Networks

Erickson Fajiculay and Chao-Ping Hsu*

Cite This: *ACS Omega* 2023, 8, 3043−3056

Read Online

ACCESS | Metrics & More | Article Recommendations | Supporting Information

ABSTRACT: Noise, or uncertainty in biochemical networks, has become an important aspect of many biological problems. Noise can arise and propagate from external factors and probabilistic chemical reactions occurring in small cellular compartments. For species survival, it is important to regulate such uncertainties in executing vital cell functions. Regulated noise can improve adaptability, whereas uncontrolled noise can cause diseases. Simulation can provide a detailed analysis of uncertainties, but parameters such as rate constants and initial conditions are usually unknown. A general understanding of noise dynamics from the perspective of network structure is highly desirable. In this study, we extended the previously developed law of localization for characterizing noise in terms of (co)variances and developed noise localization theory. With linear noise approximation, we can expand a biochemical network into an extended set of differential equations representing a fictitious network for pseudo-components consisting of variances and covariances, together with chemical species. Through localization analysis, perturbation responses at the steady state of pseudo-components can be summarized into a sensitivity matrix that only requires knowledge of network topology. Our work allows identification of buffering structures at the level of species, variances, and covariances and can provide insights into noise flow under non-steady-state conditions in the form of a pseudo-chemical reaction. We tested noise localization in various systems, and here we discuss its implications and potential applications. Results show that this theory is potentially applicable in discriminating models, scanning network topologies with interesting noise behavior, and designing and perturbing networks with the desired response.

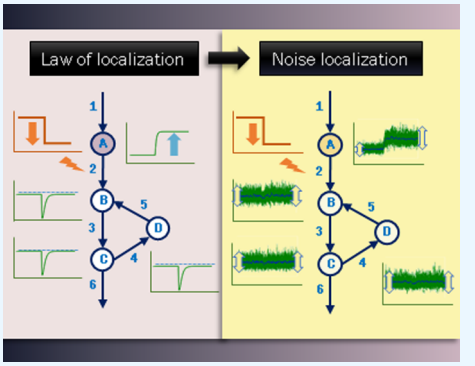

I. INTRODUCTION

Heterogeneous gene expression and dynamics have been observed in cells with identical genetic backgrounds, cultivated under the same conditions. Such uncertainty, or noise, has been studied in the context of gene regulation and phenotypic variation.[1−9] In a (bio)chemical system, especially in cells, component uncertainty can arise at the molecular level from the probabilistic nature of chemical reactions.[1] Noise can also arise from fluctuation or uncertainty in external factors, leading to the large cell-to-cell variation observed in the literature.[1,10]

Regulation of noise is crucial for species survival.[11−13] Uncontrolled noise can deteriorate vital functions of cells, especially those that require precision. Noise has also been one aspect of studies of diseases, such as cancer.[14−16] On the other hand, regulated noise, such as mechanisms that increase heterogeneity in systems, may be advantageous in coping with stress, diversifying antibodies, increasing functional heterogeneity, etc..[17−20] Understanding of the role of noise and its regulation has been growing,[21−24] resulting in applications in cancer therapy and drug design.[25−27]

Theories and computational techniques for modeling intrinsic noise have been developed, but are constantly being modified and improved. The chemical master equation (CME)[28] is a stochastic theory that accounts for the production of intrinsic noise in biochemical systems. It is a set of ordinary differential equations (ODE) that describes the state space of a system as a time-dependent probability distribution function.[29] For most systems, the CME cannot be solved analytically. An alternative approach is to perform numerical sampling using the stochastic simulation algorithm (SSA).[30] SSA is an exact realization of the CME that is very easy to implement, but simulations can be time-consuming, especially for systems of reactions of different time scales. A τ-leaping algorithm that takes large time steps has been introduced, employing statistically estimated means and variances in the reactions. It greatly reduces the computational cost compared to SSA, but it can be less accurate.[31] Some implementations that shift between SSA and τ-leaping have been developed to prevent most of the loss of accuracy.[31,32] In terms of speed, a less accurate, but faster approach than τ-leaping is the chemical Langevin equation.[33−35] With this approach, the error can be large for some systems, especially if the step size is not properly chosen.[36,37]

The study of biological noise using numerical approaches, like all dynamic simulations, requires data for initial conditions and rate constants, which can sometimes be estimated by

Received: September 22, 2022
Accepted: December 27, 2022
Published: January 11, 2023

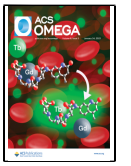

https://doi.org/10.1021/acsomega.2c06113
ACS Omega 2023, 8, 3043−3056

fitting.[38−42] However, available data are usually insufficient to constrain parameters.[43−46] In this case, one possible approach is to randomly draw parameters from a physically meaningful range and to perform simulations for all combinations of those parameters. By so doing, conclusions can be deduced based on the most probable and consistent outcome, assuming that the generally robust nature of biological systems implies considerable independence in system behavior.[47−50] This approach is time-consuming and does not necessarily generate correct results. With many possible parameter sets, sensitivity is often studied with statistical quantities only.[51−53] In any case, it is highly desirable to obtain properties of a system without knowing the actual parameters.

Linear noise approximation (LNA) has been an important tool in the study of noise, in the form of (co)variances of species in the system.[54,55] With a power expansion in the CME, LNA yields a set of ODEs for (co)variances of components. For small systems, LNA can be solved analytically, providing expressions that relate (co)variances to rate constants and initial composition.[56] LNA, to some extent, can be used to draw general conclusions, as it has been a powerful technique for deducing various factors in noise propagation.[57−60] LNA-derived noise can also be decomposed into noise contributions from individual reactions in the network.[61]

Another useful mathematical tool in the study of biological dynamics is the law of localization.[62,63] Perturbations of reaction rates, such as inhibition, knockdown, or upregulation of genes or enzymes, could promote changes in steady-state composition that can be monitored experimentally[64] and can be predicted through localization analysis. Based only on topology, a sensitivity matrix formulated by inverting the Jacobian of fluxes with appended null space of the stochiometric matrix, the law of localization predicts the overall perturbation response of a network. This theory gives rise to the concept of buffering structures, which are subnetworks of a network such that perturbation of reactions inside a buffering structure only affects species inside, while the rest of the network is unaffected. Such phenomena can be associated with systems where important compounds are under tight homeostasis and are robust to perturbations.[65] It was also reported that a large number of species in a carbon metabolic network do not respond to multiple enzyme knockouts,[64] which can be attributed to buffering structures. Buffering structures have also been applied in the study of bifurcations.[66,67] For small systems, buffering structures can be easily identified using simple rules.[63] However, the study of large systems may still rely on numerical computations, which require parameter values that can be scanned or sampled. With the law of localization, there is no need to perturb each parameter and to solve for steady-state ODE of the system repeatedly. This makes the law of localization a very efficient method for finding perturbation responses. The growing availability of multiple high-throughput (knockdown/knockout) data[68] and (cellular) perturbation screens[69] that can be compared with predicted response patterns from the law of localization may promote better network reconstruction,[70−77] model discrimination,[78,79] and network engineering.[80]

Since LNA generates a set of ODEs for (co)variances, it would be interesting to see if such ODEs can be further analyzed using the law of localization. By so doing, i.e., combining LNA with the law of localization, it becomes possible to deduce the noise response or relative change in (co)variance after perturbation of a network of reactions. In the present work, we focus on noise predicted by the law of localization in open systems. We limit our scope to open systems that allow exchange of material with the surrounding environment. These typically have at least an incoming and an outgoing flux with the surroundings. This type of system is commonly found in nature, but because the full scale of natural systems is undetermined, we can only study a portion of such systems, in which at least one component is produced via inflow, and at least one component is degraded via outflow. Systems that do not exchange molecules with their environments are sometimes called closed systems,[81] and they have a different set of constraints; thus, they require a separate set of considerations, which we plan to investigate in future work.

Here, we address the study of noise[55] by inferring noise dynamics based on network structure. We adopted the law of localization in a chemical reaction network[62] and combined it with LNA[54,82] to derive a mathematical approach that can help to infer the behavior of noise. In doing so, we can deduce a pseudo-chemical reaction that includes (co)variances. Together with a set of chemical reactions, our results provide a qualitative and quantitative picture of noise dynamics, from a simple look-up to numerical calculations. We tested our approach on selected systems, and we provide a rationale for its implications and potential applications.

II. THEORY AND METHODS

We first briefly introduce LNA and network localization in this section. Noise localization is developed by combining the two, which we describe at the end of this section.

II.I. Linear Noise Approximation. With a power expansion of the system size in the CME,[82] a linear Fokker−Planck equation[83] can be obtained, as shown in eqs 1−3

$$\frac{\partial \Pi(\boldsymbol{\xi}, t)}{\partial t} = -\sum_{i}^{N}\sum_{k}^{N} A_{i,k}\frac{\partial(\xi_k \Pi(\boldsymbol{\xi}, t))}{\partial \xi_i} + \frac{1}{2}\sum_{i}^{N}\sum_{k}^{N} [\boldsymbol{B}\boldsymbol{B}^{\mathrm{T}}]_{i,k}\frac{\partial}{\partial \xi_i}\frac{\partial \Pi(\xi, t)}{\partial \xi_k} \quad (1)$$

where

$$\boldsymbol{A} = \boldsymbol{V}\frac{\partial \boldsymbol{w}(\boldsymbol{k}, \boldsymbol{x})}{\partial \boldsymbol{x}} \quad (2)$$

and

$$\boldsymbol{B}\boldsymbol{B}^{\mathrm{T}} = \boldsymbol{V}\ \mathrm{diag}(\boldsymbol{w})\boldsymbol{V}^{\mathrm{T}} \quad (3)$$

In the equations above, $\boldsymbol{x}$ is a vector of length N describing the amounts of various chemical species in the system, $\boldsymbol{\xi}$ is a random variable equivalent to $\boldsymbol{x} - \langle \boldsymbol{x} \rangle$, $\boldsymbol{w}$ is the propensity vector, which is a function of $\boldsymbol{x}$, and the vector of rate constant $\boldsymbol{k}$, t is the time, $\boldsymbol{V}$ is the stoichiometric matrix, and Π is a probability distribution of $\boldsymbol{\xi}$. Assuming that Π follows a Gaussian distribution, eq 1 can be simplified to

$$\frac{\partial \boldsymbol{C}}{\partial t} = \boldsymbol{C}\boldsymbol{A}^{\mathrm{T}} + \boldsymbol{A}\boldsymbol{C} + \boldsymbol{B}\boldsymbol{B}^{\mathrm{T}} \quad (4)$$

where $\boldsymbol{C}$ is the covariance matrix of $\boldsymbol{x}$.

At steady state, eq 4 vanishes to zero.[54,84] For simple systems, an analytical solution to the covariance can be found, but a numerical approach is still needed for large systems.

II.II. Law of Localization in Chemical Networks. The law of localization in chemical networks[62] takes advantage of the null space of the stoichiometric matrix, which constrains changes in

https://doi.org/10.1021/acsomega.2c06113
ACS Omega 2023, 8, 3043−3056

reaction fluxes. A set of M chemical reactions among N species can be represented as a product of a stoichiometric matrix and propensities, or fluxes, as shown in eq 5

$$\frac{\mathrm{d}x_i}{\mathrm{d}t} = \sum_{j=1}^{M} V_{i,j} w_j(\boldsymbol{k}, \boldsymbol{x}), \quad i = 1, \cdots, N \tag{5}$$

The flux vector, $\boldsymbol{w}(\boldsymbol{k},\boldsymbol{x})$, is a function of the component vector $\boldsymbol{x}$, and rate constants vector $\boldsymbol{k}$, with w_j corresponding to the flux of reaction j. At steady state, eq 5 vanishes to zero. Perturbation of the jth reaction by a change in the rate constant k_{j^*} at steady state results in perturbation of $\boldsymbol{w}$, which is mathematically equivalent to

$$\frac{\delta w_j}{\delta k_{j^*}} = \frac{\partial w_j}{\partial k_{j^*}} + \sum_{i}^{N} \frac{\partial w_j}{\partial x_i} \frac{\mathrm{d}x_i}{\mathrm{d}k_{j^*}} \tag{6}$$

In considering the influence of a perturbation on reaction rates to changes in the steady states, one can consider

$$\sum_{j=1}^{M} V_{i,j} \left[\frac{\partial w_j}{\partial k_{j^*}} + \sum_{i}^{N} \frac{\partial w_j}{\partial x_i} \frac{\mathrm{d}x_i}{\mathrm{d}k_{j^*}} \right] \delta k_{j^*} = 0 \tag{7}$$

Following ref 62, a null space could exist, which is spanned by vectors $\boldsymbol{c}_z$ orthogonal to the raw vectors of $\boldsymbol{V}$, with the combination of reaction fluxes that is not constrained by the steady-state condition. Therefore, the new steady-state condition with a change in reaction rate can be written as

$$\left(\frac{\partial w_j}{\partial k_{j^*}}\right) \delta k_{j^*} + \left(\frac{\partial w_j}{\partial x_i}\right) \delta x_i = \sum_{z=1}^{Z} u_{z,j^*} c_{j,z} \tag{8}$$

where $\boldsymbol{u}_z$ denotes coefficients for the null space. Rearrangement and transposition of terms in eq 8 followed by factorization into matrix products gives us the following expression

$$\boldsymbol{S} = -\boldsymbol{A}^{-1}(e_1, \ldots, e_M) \tag{9}$$

where

$$\boldsymbol{S} = \left(\begin{array}{ccc} \delta x_1^1 & \cdots & \delta x_1^M \\ \vdots & \vdots & \vdots \\ \delta x_N^1 & \cdots & \delta x_N^M \\ \hline \mu_1^1 & \cdots & \mu_1^M \\ \vdots & \vdots & \vdots \\ \mu_Z^1 & \cdots & \mu_Z^M \end{array}\right) \tag{10}$$

and

$$\boldsymbol{A} = \left(\frac{\partial \boldsymbol{w}}{\partial \boldsymbol{x}} \middle| -\boldsymbol{c}_1, \cdots, -\boldsymbol{c}_Z\right) \tag{11}$$

In these expressions, Z is the dimension of the null space of $\boldsymbol{V}$; $\boldsymbol{S}$ is the network sensitivity, composed of $\delta\boldsymbol{x}$, which is $(\partial\boldsymbol{x}/\partial\boldsymbol{k})\delta\boldsymbol{k}$, and coefficients of the null space of $\boldsymbol{V}$, the row vector $\boldsymbol{u}_z$, respectively; $\boldsymbol{A}$ is a matrix of the derivative of $\boldsymbol{w}$ with respect to $\boldsymbol{x}$, with null space of $\boldsymbol{V}$ appended; and e_j is $(\partial w_j/\partial k_{j^*})\delta k_{j^*}$. With these manipulations, the sensitivity $\boldsymbol{S}$ yields information for network localization.

For example, in the case of knockdown or inhibition, δk_{j^*} is negative, and e_j can be assumed to be -1, making $\boldsymbol{S}$ equal to the inverse of $\boldsymbol{A}$. The network sensitivity $\boldsymbol{S}$ is a table of responses in which columns are reactions and the first N rows are chemical species. Entries in the table are either zero or simple mathematical expressions. A zero entry indicates that perturbing a particular reaction does not change the corresponding chemical species at steady state. For nonzero responses, when k_{j^*} is inhibited, the sign of the sensitivity indicates the corresponding direction of changes in the species concentration. Contrarily, when k_{j^*} is upregulated, e_j is positive in eq 9 and the fate of species upon reaction perturbation follows the same principle. The main implication of the law of localization is that response patterns exhibit localization and hierarchy. This means that perturbation of an upstream reaction does not necessarily affect downstream reactions. Buffering structures, in which perturbations can be confined, can be summarized as a metabolite and reaction subset pair, which are components with nonzero responses in a column of $\boldsymbol{S}$ and their associated reactions.

II.III. Noise Localization. We further analyze noise[55] with law of localization theory[62] for open systems, where nontrivial results of perturbation in the noise can be formulated. To formulate a network sensitivity matrix that includes noise as (co)variances for open systems at steady state, the component vector $\boldsymbol{x}$ and unique nonzero elements of the covariance matrix $\boldsymbol{C}$ are combined into vector $\boldsymbol{G}$, shown in eq 12.

$$\boldsymbol{G} = (C_{1,1}, C_{1,2}, \cdots, C_{i,j}, \cdots, C_{N,N}, x_1, \cdots, x_i, \cdots, x_N)^{\mathrm{T}} \tag{12}$$

The differential equation of $\boldsymbol{G}$ is a column vector representing unique expressions of the concatenation of eqs 4 and 5 as follows

$$\frac{\mathrm{d}\boldsymbol{G}}{\mathrm{d}t} = \begin{pmatrix} \dfrac{\mathrm{d}C_{i,j}}{\mathrm{d}t} \\ \vdots \\ \dfrac{\mathrm{d}x_i}{\mathrm{d}t} \\ \vdots \end{pmatrix}, \quad i = 1 \text{ to } N \text{ and } j = i \text{ to } N \tag{13}$$

Expansion of eqs 4 to 5 and substitution into eq 13 gives the expression

$$\frac{\mathrm{d}\boldsymbol{G}}{\mathrm{d}t} = \begin{pmatrix} g_1^{1,1} + g_2^{1,1} + g_3^{1,1} \\ g_1^{1,2} + g_2^{1,2} + g_3^{1,2} \\ \vdots \\ g_1^{i,j} + g_2^{i,j} + g_3^{i,j} \\ \vdots \\ g_1^{N,N} + g_2^{N,N} + g_3^{N,N} \\ g_4^{1} \\ \vdots \\ g_4^{i} \\ \vdots \\ g_4^{N} \end{pmatrix} \tag{14}$$

where $\boldsymbol{g}$'s are defined as

https://doi.org/10.1021/acsomega.2c06113
ACS Omega 2023, 8, 3043−3056

$$g_1^{i,j} = \sum_{l,k} V_{i,l} \frac{\partial w_l}{\partial x_k} C_{k,j} \tag{15}$$

$$\boldsymbol{g}_2 = \boldsymbol{g}_1^{\mathrm{T}} \tag{16}$$

$$g_3^{i,j} = \sum_{l,m} V_{i,l}\, \mathrm{diag}(w)_{l,m} V_{j,l} \tag{17}$$

and

$$g_4^{\,i} = \sum_j V_{i,j} w_j \tag{18}$$

Noting that $\boldsymbol{w}$ is a function of $\boldsymbol{x}$ and $\boldsymbol{k}$, we can simplify the expression to a linear combination of $\boldsymbol{w}$ and $\boldsymbol{w}'\boldsymbol{C}$, where $\boldsymbol{w}'$ is the derivative of $\boldsymbol{w}$ with respect to $\boldsymbol{x}$.

$$\frac{\mathrm{d}\boldsymbol{G}}{\mathrm{d}t} = \begin{pmatrix} \sum_{l,k} V_{j,l} w'_{l,k} C_{k,i} + \sum_{l,k} V_{i,l} w'_{l,k} C_{k,j} + \sum_l V_{i,l} V_{j,l} w_l \\ \vdots \\ \sum_j V_{i,j} w_j \\ \vdots \end{pmatrix} \tag{19}$$

Equation 19 can be simplified into a form similar to eq 5 as follows

$$\frac{\mathrm{d}\boldsymbol{G}}{\mathrm{d}t} = \boldsymbol{Q}\boldsymbol{z}(\boldsymbol{k}, \boldsymbol{x}, \boldsymbol{C}) \tag{20}$$

and

$$\boldsymbol{Q} = \begin{pmatrix} \eta V_{1,1}, & \cdots & , V_{1,M} V_{1,M} \\ \vdots & \ddots & \vdots \\ \eta V_{N,1} & \cdots & V_{N,M} V_{N,M} \end{pmatrix} \tag{21}$$

and

$$\boldsymbol{z} = (w'_{1,1} C_{1,1}, w'_{1,2} C_{2,1}, \cdots, w'_{l,k} C_{k,i}, \cdots, w'_{M,N} C_{N,N}, w_1, \cdots, w_M)^{\mathrm{T}} \tag{22}$$

where $\boldsymbol{Q}$ and $\boldsymbol{z}$ are a pseudo-stoichiometric matrix and a pseudo-propensity or a pseudo-flux vector, respectively. Entries in the columns for a row of $\boldsymbol{Q}$ can be repeated if there is more than one nonzero element in the summation over index k in eq 19. When $i = j$, similar terms will appear for a particular l, k value giving rise to a factor 2 in some terms. Therefore, the η in eq 21 is 2 when $i = j$ in eq 19, otherwise $\eta = 1$. The pseudo-propensity vector $\boldsymbol{z}$ in eqs 20 and 22 is composed of functions of $\boldsymbol{k}$, $\boldsymbol{x}$, and $\boldsymbol{C}$. Since eq 20 resembles a regular differential equation for chemical reactions, we can deduce a pseudo-chemical reaction from eq 20 that includes the covariance as species. This pseudo-chemical reaction describes the flow of noise in the system from the source to the reservoir. An algorithm that extracts the pseudo-chemical reaction and factorizes a system of ODEs into a form similar to eq 20 is provided in the following link; "https://github.com/efajiculay/NoiseLocalization."

Following this derivation and using the law of localization, we derive a pseudo-network sensitivity matrix $\boldsymbol{\mathcal{S}}$ similar to eq 9 that includes the noise terms as species. This time, the effect of perturbation on the (co)variance is also explained. Localization and perturbation hierarchies with both chemical species and (co)variance terms can be deduced from $\boldsymbol{\mathcal{S}}$. We can also adopt the metabolite subset pair from ref 62 to identify buffering structures in the pseudo-chemical reaction network and can infer bifurcation in noise similar to ref 66.

From eqs 9 and 11, the corresponding $\boldsymbol{A}$ and $\boldsymbol{S}$ matrix for noise localization is as follows

$$\begin{aligned} \boldsymbol{\mathcal{A}} &= \left(\frac{\partial \boldsymbol{z}}{\partial \boldsymbol{G}} \middle| -\boldsymbol{c}'_1, \cdots, -\boldsymbol{c}'_Z \right) \\ &= \left(\frac{\partial \boldsymbol{z}}{\partial \boldsymbol{C}_1}, \cdots, \frac{\partial \boldsymbol{z}}{\partial \boldsymbol{C}_N} \middle| \frac{\partial \boldsymbol{z}}{\partial \boldsymbol{x}} \middle| - \boldsymbol{c}'_1, \cdots, -\boldsymbol{c}'_Z \right) \end{aligned} \tag{23}$$

and

$$\boldsymbol{\mathcal{S}} = \begin{pmatrix} \boldsymbol{\delta C} \\ \boldsymbol{\delta x} \\ \boldsymbol{u} \end{pmatrix} = \left(\begin{array}{ccc} \delta C_{11}^1 & \cdots & \delta C_{11}^M \\ \vdots & \cdots & \vdots \\ \delta C_{ij}^1 & \vdots & \delta C_{ij}^M \\ \vdots & \cdots & \vdots \\ \delta C_{NN}^1 & \cdots & \delta C_{NN}^M \\ \hline \delta x_1^1 & \cdots & \delta x_1^M \\ \vdots & \vdots & \vdots \\ \delta x_N^1 & \cdots & \delta x_N^M \\ \hline \mu_1^{\,1} & \cdots & \mu_1^{\,M} \\ \vdots & \vdots & \vdots \\ \mu_Z^{\,1} & \cdots & \mu_Z^{\,M} \end{array} \right) \tag{24}$$

. As in the network localization, $\boldsymbol{c}'$ is the null space of the new stoichiometric matrix $\boldsymbol{Q}$, and $\boldsymbol{u}$ is now composed of row vectors for the coefficient of the null space. The pseudo-sensitivity matrix can be expressed as

$$\boldsymbol{\mathcal{S}} = -\boldsymbol{\mathcal{A}}^{-1}(\boldsymbol{e}'_1, \cdots, \boldsymbol{e}'_M) \tag{25}$$

where e'_j is negative (-1) for inhibition and positive $(+1)$ for activation or upregulation. Noise localization is similar to the law of localization, and the response (increase, decrease, or unchanged) can be predicted from the sensitivity matrix, except for cases in which the sign of the expression can be both negative and positive.

Equation 25 offers a way to perform noise localization analysis, which provides information on the perturbation response of system (co)variances. However, multiple columns in $\boldsymbol{\mathcal{S}}$ can be associated with the same rate constant. This problem can be resolved by a linear combination of columns controlled by the same parameter. Column labels in $\boldsymbol{\mathcal{S}}$ are pseudo-propensities and row labels are pseudo-components. A particular rate constant k_j can be present in more than one column label. For a pseudo-component in each row, the effective response for a perturbation of k_j is the sum of all columns in that row where k_j appears in the column label multiplied by the steady-state value of the column label, as shown in the following equation

https://doi.org/10.1021/acsomega.2c06113
ACS Omega 2023, 8, 3043−3056

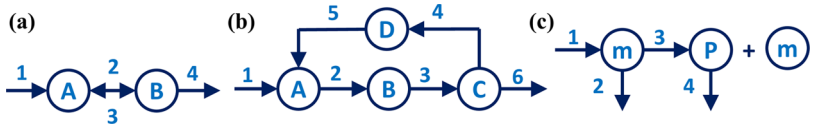

Figure 1. Monomolecular open systems analyzed using noise localization. Reactions are labeled with numbers and components with letters. (a) Two-state reversible reaction in a linear chain. (b) This example is a four-state reaction with a cycle constructed based on ref 62. (c) Simple gene regulation model.

$$\boldsymbol{S}^{e} = \boldsymbol{SH}, \text{ where } H_{i,j} = \begin{cases} z_i, & \text{if } \dfrac{\partial z_i}{\partial k_j} \neq 0 \\ 0, & \text{if } \dfrac{\partial z_i}{\partial k_j} = 0 \end{cases} \tag{26}$$

This scaling or weighting is necessary for numeric noise localization to match the linear noise approximation (LNA)-independent perturbation responses. The pseudo-propensities $\boldsymbol{z}$ serve as the probability or weight of the response.

II.III.I. Variance Response. With eqs 23−26 we can analyze the localization structure of variances and covariances. However, we find that it is helpful to summarize the variance first since there are cases in which we can infer the variance via the law of localization.

Under mass-action kinetics, linear open systems consist of two types of elementary steps, a zero-order production reaction, and a first-order degradation or transformation reaction. Knowing that $\boldsymbol{z}$ is a function of $\boldsymbol{w}$ and $\boldsymbol{w}'\boldsymbol{C}$, the term $\partial \boldsymbol{z}/\partial \boldsymbol{G}$ from eq 23 can provide the behavior of species and variances. For first-order reactions, $\boldsymbol{w}$ is composed of linear products of $\boldsymbol{k}$ and $\boldsymbol{x}$, making $\boldsymbol{w}'$ a function of $\boldsymbol{k}$ only. This makes $\partial \boldsymbol{z}/\partial \boldsymbol{G}$ for the variance $C_{i,i}$ and the species x_i equal or $\partial \boldsymbol{w}/\partial x_i = \partial \boldsymbol{w}'\boldsymbol{C}/\partial C_{i,i} = w'_i$. Upon inversion of the $\mathcal{A}$ matrix, which is a sparse matrix, these two derivatives give the same result, which indicates that the response of the variance $C_{i,i}$ and the species x_i is the same. For zero-order reactions, $\boldsymbol{w}$ is only a function of $\boldsymbol{k}$, and such terms in $\boldsymbol{w}'$ equal zero. This means that $\partial \boldsymbol{z}/\partial \boldsymbol{G}$ is zero for variances and species making them behave in the same way. Therefore, when the form of $\boldsymbol{w}$ is either zero (independent of $\boldsymbol{x}$) or first order (monomolecular) with respect to x_i, the following relation holds

$$\frac{\partial \boldsymbol{z}}{\partial C_{ii}} = \frac{\partial \boldsymbol{z}}{\partial x_i}, \quad i = 1 \text{ to } N \tag{27}$$

For systems in which eq 27 holds, the response of $C_{i,i}$ with respect to reaction perturbation follows that of x_i. In this case, the response of the variance can be deduced directly from the law of localization following the sign of the sensitivity matrix in eq 9.

If the form of $\boldsymbol{w}$ is complex with respect to x_i, a noise localization sensitivity matrix is required to describe the fate of $C_{i,i}$ since there is no assurance that eq 27 still holds. For example, $\boldsymbol{w}$ can include Hill-type expressions and other nonlinear functions arising from multimolecular reactions. In this case, rate constant perturbation can be inferred from eq 25.

In an open system, concentration perturbation generally does not affect the variance. However, for nonlinear systems that exhibit multiple stable fixed points, concentration perturbation might allow shifting between fixed points giving complicated perturbation responses. This, however, is not currently accounted for.

The response of variance can also be used to estimate the most likely response of the coefficient of variation (CV) defined as $100\sqrt{\text{var}(x_i)}/\langle x_i \rangle$. As long as $\text{var}(x_i)$ is less than $\langle x_i \rangle^2$, CV will decrease as $\langle x_i \rangle$ increases. For Poisson processes, $\text{var}(x_i) = \langle x_i \rangle$ and deviation from Poisson is very unlikely to result in $\text{var}(x_i) \geq \langle x_i \rangle^2$. In general, the fano factor or $\text{var}(x_i)/\langle x_i \rangle$ is a small number. This set of statements suggests that if $\text{var}(x_i)$ and $\langle x_i \rangle$ increase, then $\text{CV}(x_i)$ most likely decreased. If $\text{var}(x_i)$ and $\langle x_i \rangle$ decreases $\text{CV}(x_i)$ most likely increased. Under certain conditions, for nonlinear cases, opposite responses between $\text{var}(x_i)$ and $\langle x_i \rangle$ might be observed. If $\text{var}(x_i)$ decreased and $\langle x_i \rangle$ increased, $\text{CV}(x_i)$ definitely decreased. If $\text{var}(x_i)$ increased and $\langle x_i \rangle$ decreased, $\text{CV}(x_i)$ certainly increased. For instance, where either $\text{var}(x_i)$ or $\langle x_i \rangle$ has no response, $\text{CV}(x_i)$ can still be logically predicted since $\text{CV}(x_i)$ is directly proportional to $\sqrt{\text{var}(x_i)}$ and inversely proportional to $\langle x_i \rangle$. Finally, if both $\text{var}(x_i)$ and x_i have no response, $\text{CV}(x_i)$ surely has no response.

II.III.II. Covariance Response. Since eq 25 involves the inverse of a large matrix, it is cost-effective to take advantage of cases in which the steady-state value of the covariance is zero. In open systems, the covariance $C_{i,j\neq i}$ is zero at steady state for zero-order and first-order (monomolecular) reactions in which reactants or products are no more than one species. This was derived in ref 81 through CME, in which the probability of species becomes a product of a Poisson distribution at steady state. The mean and variance of a Poisson random variable are equal and the covariance between independent Poisson random variables is zero. However, the derivation in ref 81 does not account for monomolecular systems that include autocatalysis and splitting of reactants, i.e., production of more than one product in a monomolecular reaction. For such systems, if the sum of the rows in each column in eq 2 is either zero or negative, then all covariances are zero. Otherwise, there is no assurance that all covariances are zero. The simple gene regulation model in Figure 1c demonstrated in Section III.I is one such exception. It is a linear system with nonzero covariance.

Here we summarize our current understanding of cases with nonzero covariance:

1. $C_{i,j\neq i}$ is nonzero for systems in which the total number of molecules is conserved. This is because a mathematical relationship between any two species can be defined by exploiting the mass−balance relationship.

2. $C_{i,j\neq i}$ can be nonzero if x_i and x_j are co-produced or co-consumed either directly or indirectly. This is usually observed in multimolecular reactions, disintegration reactions, breakdown or dissociation reactions, etc.

3. $C_{i,j\neq i}$ can be nonzero if the system is described by a complicated propensity function containing functions other than constants and first-order terms.

For nonzero covariance, the ODE should be added to the list of ODEs in eq 13 to reflect their perturbation behavior in the pseudo-sensitivity matrix.

https://doi.org/10.1021/acsomega.2c06113
ACS Omega 2023, 8, 3043−3056

Table 1. Perturbation Effect in a Two-State, Reversible, Open System[a]

		parameters						LNA estimate (rounded)				
row no.	case	A_0	B_0	k_1	k_2	k_3	k_4	A	B	C_{AA}	C_{AB}	C_{BB}
1	original	100	10	200	50	55	20	15	10	15	0	10
2	$+A_0$	500	10	200	50	55	20	15	10	15	0	10
3	$+B_0$	100	200	200	50	55	20	15	10	15	0	10
4	$+k_1$	100	10	250	50	55	20	18.75	12.5	18.75	0	12.5
5	$+k_2$	100	10	200	100	55	20	7.5	10	7.5	0	10
6	$+k_3$	100	10	200	50	90	20	22	10	22	0	10
7	$+k_4$	100	10	200	50	55	200	5	1	5	0	1

[a]+ indicates an increase in value compared to row 1.

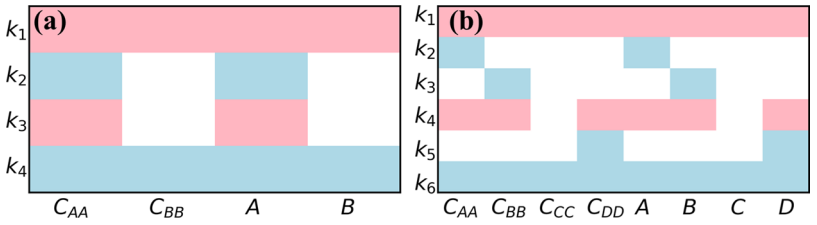

Figure 2. Summary of the perturbation response for the monomolecular open systems in Figure 1a,b using symbolic noise localization. Pink denotes a reduction in magnitude. White indicates no effect, and blue represents an increase in magnitude. $C_{i,i}$ corresponds to the variance of species i, and k_i's are rate constants.

III. RESULTS AND DISCUSSION

In the following section, perturbation analysis using noise localization is applied to selected systems and compared to LNA with rate constant perturbations or to direct evaluation of the analytical expression whenever applicable. The result is tabulated where dynamics of noise upon perturbations are easily seen. All perturbations applied in this work are inhibitions. The effect of upregulation can be deduced by flipping the signs observed from the response obtained. Section III.I focuses on monomolecular systems in which all mass-action kinetics are either zero or first-order reactions. Discussions of multimolecular systems follow in Section III.II. Section III.III is an application of noise localization to the glycolysis and TCA cycle of *Escherichia coli*. Codes and derivation for each example can be found at https://github.com/efajiculay/NoiseLocalization.

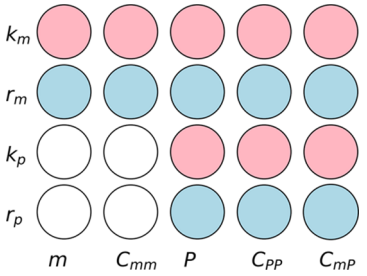

Figure 3. Perturbation response for the simple gene regulation model in Figure 1c using numeric noise localization summarized for 100 samples. Pink stands for a reduction in magnitude. White indicates no effect, and blue represents an increase in magnitude. $C_{i,i}$ corresponds to the variance of species i. $C_{i,j}$ corresponds to the covariance between species i and j. k_m and r_m are the production and degradation rate of the mRNA m, k_p is the rate of translation from mRNA to protein P, and r_p is the degradation rate of P. The rate constants and initial composition were sampled uniformly, between the ranges of 80−200 and 0−10, respectively. Responses between $\pm 1.0 \times 10^{-10}$ are regarded as zero.

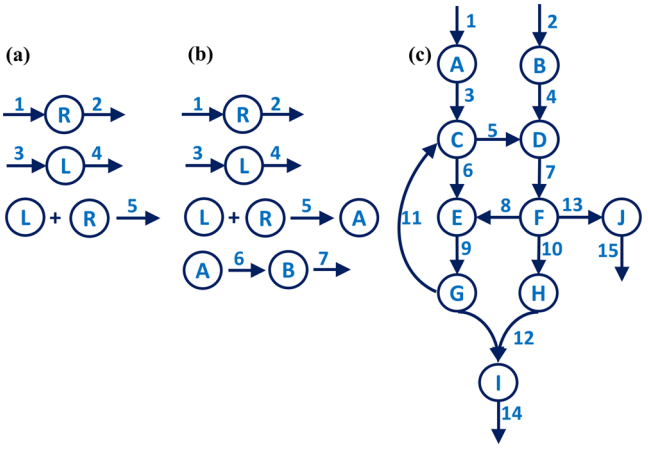

Figure 4. Hypothetical examples of bimolecular open systems. (a) Bimolecular reaction in which both components experience production and degradation, and binding of the two molecules leads to removal. (b) Here, an additional monomolecular reaction is included in the system depicted in (a). (c) Complicated monomolecular reaction with a bimolecular reaction at the end, constructed based on ref 62.

III.I. Monomolecular Systems. Figure 1 shows some examples of monomolecular systems. These types of systems are generally linear, involve zero and first-order reactions, and may have an analytical solution for the network sensitivity matrix under noise localization.

The two-state reversible reaction shown in Figure 1a is a typical monomolecular open system. Perturbation of the initial composition and reaction rates for this system are summarized in Table 1. The initial amount of each component does not affect the magnitude of steady-state composition and noise. The covariance between A and B is zero in all conditions, as the reactions have at most one species of reactant or product, as discussed in the previous section. If we decompose the noise using the method described in ref 61, reactions 2 and 3 contribute negatively to the covariance, but reactions 1 and 4 cancel those contributions. This is because the total number of

https://doi.org/10.1021/acsomega.2c06113
ACS Omega 2023, 8, 3043−3056

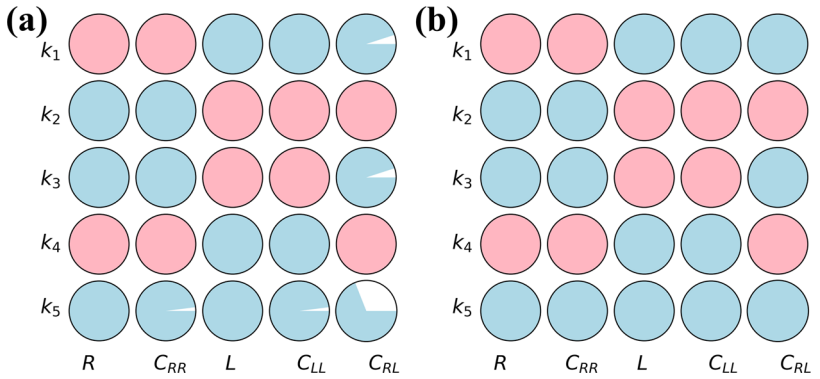

Figure 5. Perturbation responses for multimolecular open systems in Figure 4a using numeric noise localization, summarized for 100 samples. The rate constants and initial composition were uniformly sampled between the ranges of 80−200 and 0−10, respectively. Pink stands for a reduction in magnitude. White indicates no effect, and blue represents an increase in magnitude. $C_{i,i}$ corresponds to the variance of species i. $C_{i,j}$ corresponds to the covariance between species i and j. k_i's are rate constants. (a) Responses between $\pm 1.0 \times 10^{-3/2}$ are regarded as zero. (b) Responses between $\pm 1.0 \times 10^{-10}$ are regarded as zero.

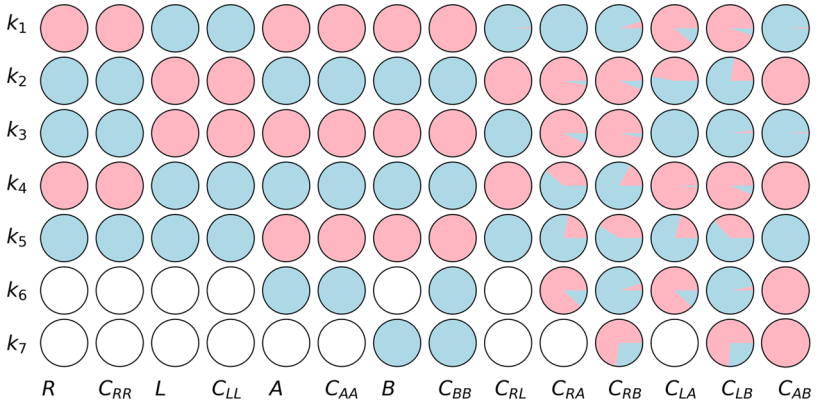

Figure 6. Perturbation dynamics for the multimolecular open systems in Figure 4b using numeric noise localization summarized for 100 samples. The rate constants and initial composition were uniformly sampled between the ranges of 80−200 and 0−10, respectively and responses between $\pm 1.0 \times 10^{-10}$ are regarded as zero. Pink stands for a reduction in magnitude. White indicates no effect, and blue represents an increase in magnitude. $C_{i,i}$ corresponds to the variance of species i. $C_{i,j}$ corresponds to the covariance between species i and j. k_i's are rate constants.

species at steady state is constantly disturbed by the firing of all reactions, making it a random variable and destroying coupling between species. The same zero-covariance also holds in the system depicted in Figure 1b.

Figure 2 includes a summary of the resulting sensitivity matrix for systems in Figure 1a,b. The perturbation effect on these components matches the variance since those systems are monomolecular. The sensitivity matrix is also sparse. For example, in (a), inhibition of k_2 or k_3 only affects A and C_{AA}. In (b), inhibition of k_2 affects A and C_{AA}, k_3 affects B and C_{BB}, and k_4 affects A, B, D, C_{AA}, C_{BB}, and C_{DD}. Under the chosen inhibition of the rate constant in each row, buffering structure can be obtained with the pseudo-components that respond in each column, as in the law of localization.[62] These structures confine the effects of perturbation, for both components and variances. In this case, the buffering structure is a consequence of the fact that at steady state, total inflow is equal to total outflow. With a perturbed rate constant, the system regains flux balance via increased or decreased quantities of nearby components, which is also reflected in the noise.

The simple gene regulation model shown in Figure 1c is special because it is a lumped reaction. The actual mechanism would involve many elementary steps, some of which are multimolecular reactions. In reaction 3, where m appears to form P and m, it is not m that forms P, but m serves as a pattern or template in the synthesis of P. The sum of the columns of eq 2 for this system includes positive terms, which imply that some covariances may not be zero.

Figure 3 is a summary of the distribution of responses for Figure 1c, using numeric noise localization. Responses of the variance match those of corresponding species and covariances have a nonzero response with the same direction of changes in each row as P. We note that C_{mp} is not zero since production of P is correlated with m in this model. In this system, the exact direction of the response can be predicted with a high level of confidence.

III.II. Multimolecular Systems. Multimolecular systems are generally nonlinear, making noise response inference complicated, and often analytically intractable. One simplification is to omit the zero-covariance term in eq 13, as discussed in the previous section. However, for multimolecular systems, it is difficult to judge whether a covariance term is zero. A solution to this is to sample random parameters and perform numeric noise localization. In this case, a range $-\nu$ to $+\nu$ needs to be defined, in which ν is a small threshold within a number to be considered zero. Responses from eq 25 need to be rescaled with the columns or pseudo-propensities that serve as weights of the responses. This is to reduce the effect of nonzero responses associated with very low fluxes. Responses associated with very low steady-state pseudo-component values in each row can be considered as

https://doi.org/10.1021/acsomega.2c06113
ACS Omega 2023, 8, 3043−3056

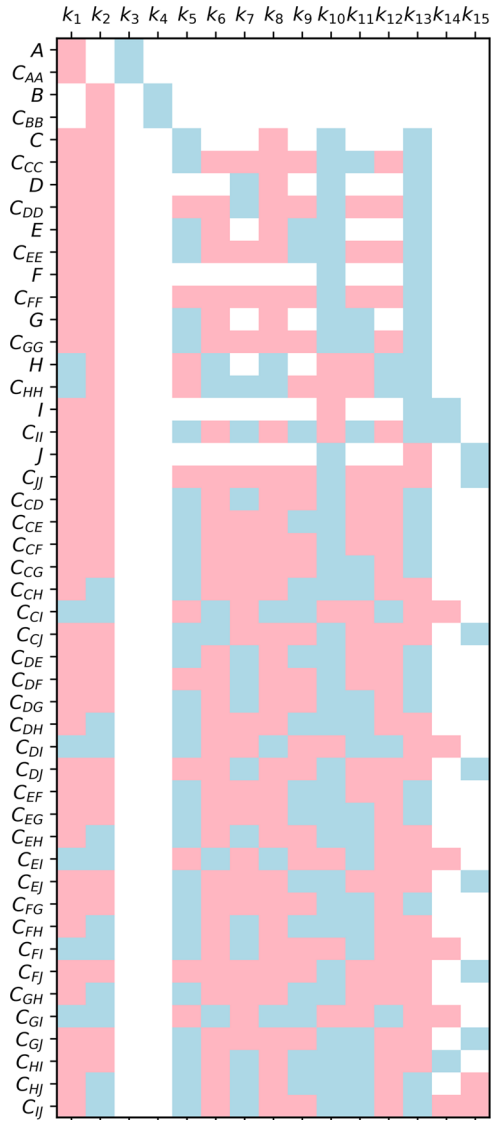

Figure 7. Most probable perturbation response for multimolecular open systems in Figure 4c using numeric noise localization summarized for 100 samples. Pseudo-components with no response in any perturbation are removed. The rate constants and initial composition were uniformly sampled between the ranges of 80−200 and 0−10, respectively, and responses between $\pm 1.0 \times 10^{-10}$ are regarded as zero. Pink stands for a reduction in magnitude. White indicates no effect, and blue represents increases in magnitude. $C_{i,i}$ corresponds to the variance of species i. $C_{i,j}$ corresponds to the covariance between species i and j. k_i's are rate constants.

zero, or that row can be omitted. This is because even if they do respond to perturbation, the effect is negligible and indistinguishable from no effect. The detail of the rescaling is reflected in eq 26 and mentioned in step 10 of the steps in noise localization in the Supporting Information.

The existence of multiple fixed points is also likely to cause problems by introducing more uncertainty into predicted noise dynamics upon perturbation. Each fixed point may have different noise dynamic behavior and some random initial conditions or small perturbations may switch between any stable, fixed points.

This subsection focuses on the use of noise localization in analysis of multimolecular open systems (Figure 4). The first two systems differ only slightly in topology and the last system is an example from the law of localization.[62] Those systems are chosen to compare different complexities of bimolecular open systems. The system in Figure 4a focuses on a simple bimolecular reaction. Figure 4b captures the effect of an upstream bimolecular reaction on a downstream monomolecular system. Finally, Figure 4c shows the effect of a bimolecular reaction on upstream monomolecular reactions.

The system shown in Figure 4a is small enough to calculate steady-state analytical expressions for pseudo-components. In eqs 28−30, the steady-state expression for L, R, and C_{LR} is provided. The noise expression for C_{LL} and C_{RR} is highly dependent on L and R, respectively, but is not shown.

$$L = \frac{k_3k_5 - k_1k_5 - k_2k_4}{2\,k_2k_4} \pm \frac{\sqrt{(k_1k_5 + k_2k_4 - k_3k_5)^2 + 4k_2k_3k_4k_5}}{2\,k_2k_4} \tag{28}$$

$$R = \frac{k_1 - k_3 + k_4L}{k_2} \tag{29}$$

$$C_{LR} = -\frac{k_5(LRk_1k_5 + LRk_3k_5 + Lk_1k_4 + Rk_2k_3)}{2(Lk_4k_5 + Rk_2k_5 + k_2k_4)(Lk_5 + Rk_5 + k_2 + k_4)} \tag{30}$$

From the expressions above, it is clear that pseudo-components are highly dependent on parameters and are expected to respond to perturbation of any parameters. Equation 28 suggests two possible solutions that are expected from the quadratic term introduced into the propensity by the bimolecular elementary step. In this system, one of the solutions gives a positive L, which is the physically meaningful solution.

The most probable perturbation response of the system, depicted in Figure 4a, is summarized in Figure 5 at two zero thresholds, $\pm 1.0 \times 10^{-3/2}$ and $\pm 1.0 \times 10^{-10}$. The appearance of a white response in (a) is due to the loose cutoff, which suggests that the choice of response cutoff range is crucial. There is no white response in (b), which is correct, based on eqs 28−30. Therefore, we believe that the cutoff chosen in (b) is strict enough for numeric tests.

Figure 6 summarizes the distribution of response patterns for the system depicted in Figure 4b. Response patterns of the variances C_{RR}, C_{LL}, C_{AA}, and C_{BB}, are matched to those of species, R, L, A, and B, except under perturbation from k_6, in which the responses of C_{BB} and B are different. Species B has zero response, which can be confirmed by the steady-state solution that is independent of k_6. However, interestingly, upon inhibition of k_6, the noise strength on B, C_{BB}, increases. In other words, with inhibition of k_6, the mean concentration of B remains the same, but the dispersion is increased. We have confirmed the positive response using numeric and semi-analytical LNA, and this is a rather nonintuitive outcome from a system that contains a bimolecular reaction. Noise localization can be used in the search or screening of such behaviors, which can be utilized in the design of networks with robust steady-state composition and desired noise behavior.

Species A and B form a buffering structure downstream of the bimolecular reaction (Figure 6), in which perturbation of k_6 and k_7 yields results expected from the law of localization. Some of the covariances appear to be a mixing of responses of the species involved. For instance, C_{RA} under k_4 perturbation has a nonzero distribution that appears separately in either R and A alone. Most

https://doi.org/10.1021/acsomega.2c06113
ACS Omega 2023, 8, 3043−3056

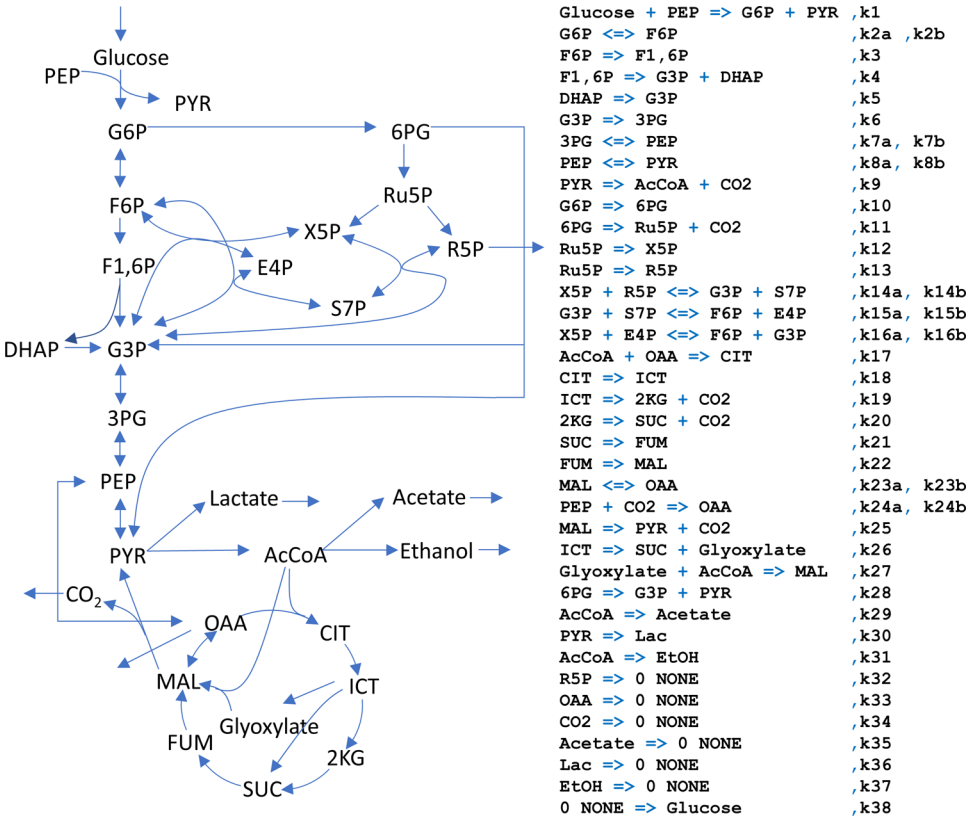

Figure 8. Glycolysis and TCA cycle of *E. coli*. This network is constructed based on refs 62, 63, and 85 and the associated reactions are written in BioSANS[56] software topology format. Exact names of each species in the network are provided in Section S3 in the Supporting Information. k_i's are rate constants with the subscript *a* or *b* corresponding to forward and backward reactions for reversible steps.

covariances have nonzero responses, which indicates that the presence of a bimolecular step couples most components. The bimolecular reaction k_5 also affects all components and their (co)variances, including upstream and downstream components.

The system shown in Figure 4c is composed of an upstream monomolecular structure with nested topologies, a high degree of branching, and a downstream bimolecular reaction. This system is expected to show complex behavior. Figure 7 shows the most probable outcome for the perturbation of reactions in Figure 4c using numeric noise localization. We have verified that the patterns shown are in good agreement with independent LNA simulations. The result is consistent with the law of localization for species *A*, *B*, *C*, *D*, *E*, *F*, *G*, *H*, *I*, and *J*. Perturbation of k_3 and k_4 is confined to *A* and *B*, which are monomolecular buffering structures and did not affect any pseudo-components except their substrate, C_{AA} and *A* for k_3 and C_{BB} and *B* for k_4. Perturbation of k_{14} and k_{15} also shows significant buffering since their substrates are also monomolecular buffering species. The perturbation response of $C_{A,j}$ (omitted in the figure) and $C_{B,j}$ (omitted in the figure) where *j* is any of the species, matches what is expected from Poisson behavior in which covariances are zero and variances match the species response. Other noise terms show greater deviation from Poisson behavior, but follow Poisson behavior in at least one of the perturbations.

In Figure 7, there are several interesting cases of patterns of pseudo-components. For example, if we compare species *C* and the corresponding variance C_{CC}, *C* does not respond to inhibition of k_6, k_7, k_9, k_{11}, and k_{12}, but C_{CC} has a nonzero response. Similar cases are also observed for other pairs of pseudo-components such as *D* and C_{DD}, *F* and C_{FF}, etc. Since the bimolecular reaction is downstream of *C*, *D*, and *F*, these differences in perturbation behavior suggest that a downstream multimolecular reaction can alter the noise response of upstream components.

III.III. Glycolysis and TCA Cycle. In this subsection, noise localization is used in modeling the perturbation response to the glycolysis and TCA cycle of *E. coli*.[62,63,85] The network consists of 28 species and 46 reactions giving 406 unique (co)variances with a total of 434 pseudo-components. Figure 8 shows a graphical representation of the network in the left panel and associated reactions in the right panel. This system involves monomolecular, bimolecular, reversible reactions and nested topologies. The full name of the species in the network is provided in Section S3 in the Supporting Information.

Figure 9 summarizes the response pattern for the glycolysis and TCA cycle of *E. coli* using (a) Noise localization and (b) LNA with parameter perturbations. Response patterns are in good agreement with an overall match of 98.4%, based on tile colors. The discrepancy is mainly because noise localization is under the assumption of infinitesimal perturbation, whereas with parameter perturbation, LNA uses actual perturbation of each parameter. As the perturbation in LNA approaches zero, the result will be closer to what we can get from noise localization. This is a limitation of noise localization in a realistic scenario in which the actual perturbation is unknown and can be large. However, noise response predicted using noise localization is still quite good under large perturbation, as can be seen in Figure 10. As the strength of inhibition increases from right to left along the *x*-axis (reverse direction), the % match between the responses of noise localization and LNA with parameter

https://doi.org/10.1021/acsomega.2c06113
ACS Omega 2023, 8, 3043−3056

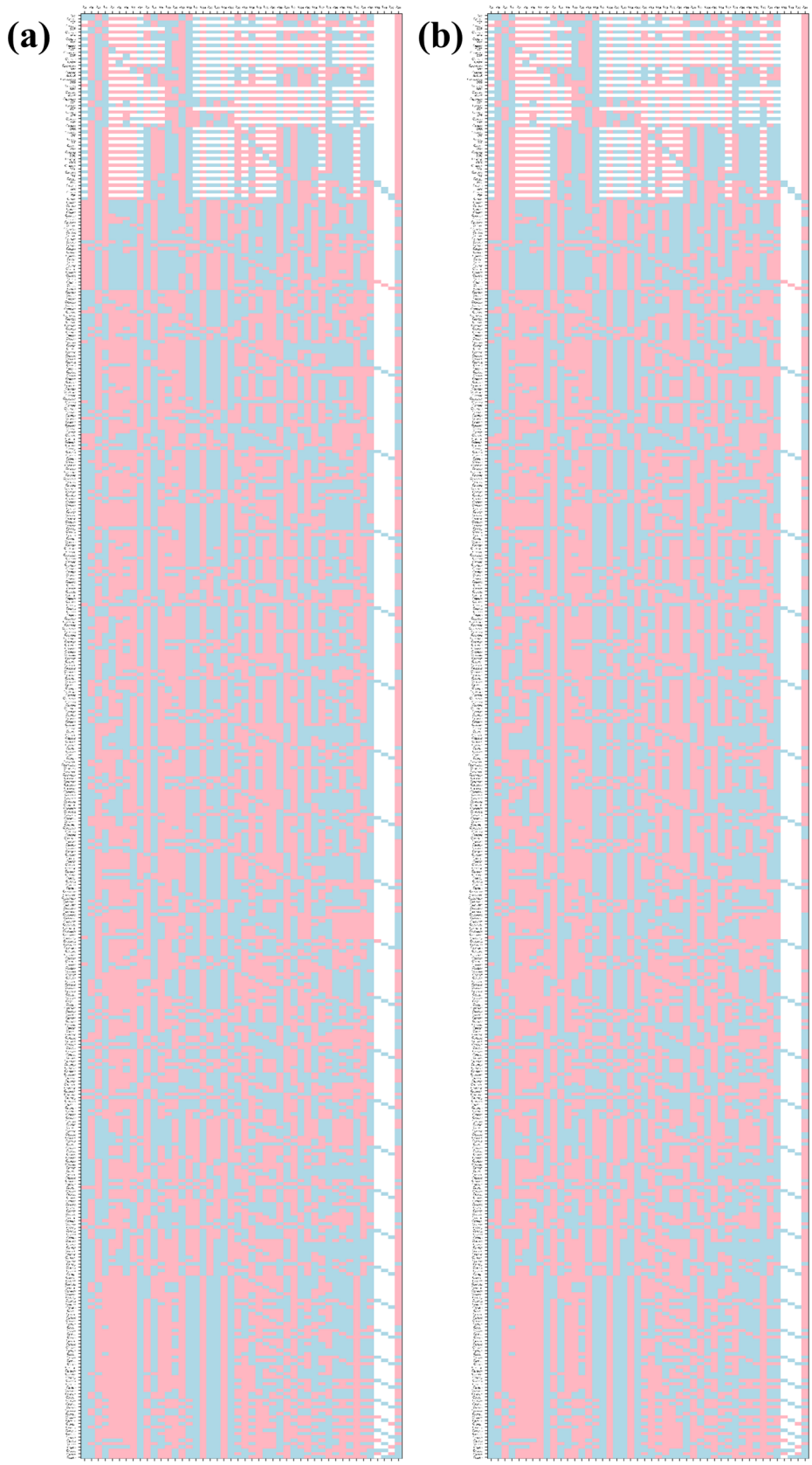

Figure 9. Most probable perturbation response of the glycolysis and TCA cycle of *E. coli* summarized for 100 samples. The rate constants and initial composition were uniformly sampled between the ranges of 80−200 and 0−10, respectively. Pink stands for a reduction in magnitude. White indicates no effect, and blue represents an increase in magnitude. Responses between $\pm 1.0 \times 10^{-10}$ are regarded as zero. $C_{i,i}$ corresponds to the variance of species *i*. $C_{i,j}$ corresponds to the covariance between species *i* and *j*. k_i's are rate constants. (a) Result of noise localization. (b) Result using LNA with individual parameters perturbed.

https://doi.org/10.1021/acsomega.2c06113
ACS Omega 2023, 8, 3043−3056

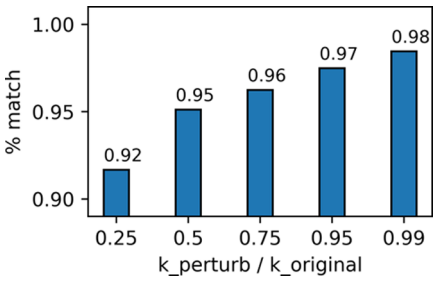

Figure 10. Effect of perturbation strength on the accuracy of predicted responses. *k*_original and *k*_perturb are the rate constants before and after perturbations, respectively; % match is the ratio of the number of responses that noise localization correctly predicts compared to responses predicted using LNA with parameter perturbations.

perturbation drops, but still above 90%. Moreover, noise localization is faster compared to LNA with parameter perturbation, especially for very large systems. In this system, noise localization is twice as fast as LNA with parameter perturbation when both methods are using multiprocessing. The difference in speed is expected to grow exponentially with system size and as the number of cores for parallel runs becomes exhausted.

Figure 11 shows the most probable perturbation response of the metabolites in Figure 8 under the perturbation of rate constants in each column. This response pattern matches what can be predicted using the law of localization. The corresponding variance response is shown in Figure 12. Even if the metabolite response is sparse, the covariance response is not. For nonlinear systems such as the glycolysis and TCA cycle of *E. coli*, the variance does not always respond the same way as the species. This result indicates that inclusion of the (co)variance response provides more discrimination power when evaluating network topologies.

Numeric noise localization provides a way to obtain the most probable response to reaction perturbation without the need to perturb each parameter. It is an efficient way to analyze a network, especially compared to numeric propagations such as SSA and SSA-derived algorithms for perturbation behavior. It is also better than performing LNA with N parameter perturbation, which entails performing $N + 1$ separate LNAs per sampled parameter.

Being able to quickly obtain the response patterns of both species concentrations and their associated noise is beneficial for inferring the reaction network of a system, a highly desirable, but difficult task. Ideally, a good model should have predicted dynamics, together with a perturbation profile that is highly consistent with experimental results. With our approach, a fast test over many different possible network structures becomes much more feasible. Noise/uncertainty can also be derived from single-cell assays, reporter-based methods, flow cytometry experiments, etc. If these were obtained by perturbing one or several components that affect the flux or rates, our approach offers more insight from the data by testing a great number of possible networks. With modern databases such as Library of Integrated Network-Based Cellular Signatures (LINCS[69]), KnockTF,[68] Human Metabolome Database,[86] etc., reverse engineering or inference of the true network and pathways will eventually become feasible, and we expect that inference from noise behavior, such as our present work, offers additional clues and constraints in the process.

IV. CONCLUSIONS

In this work, we show how qualitative and quantitative noise dynamics can be inferred by exploiting LNA and the law of localization together. The noise localization scheme we developed relies on the sensitivity matrix, which summarizes perturbation without the need to perturb parameters. It provides a way to capture the response in noise, under a perturbation of reaction rates, which can be very efficient compared to traditional approaches that require both parameter sampling and numerical perturbation.

Using the method presented here, variances and covariances in both monomolecular and multimolecular systems can be studied. Monomolecular open systems generally provide concrete answers regarding the fate of pseudo-components in response to perturbation. On the other hand, multimolecular

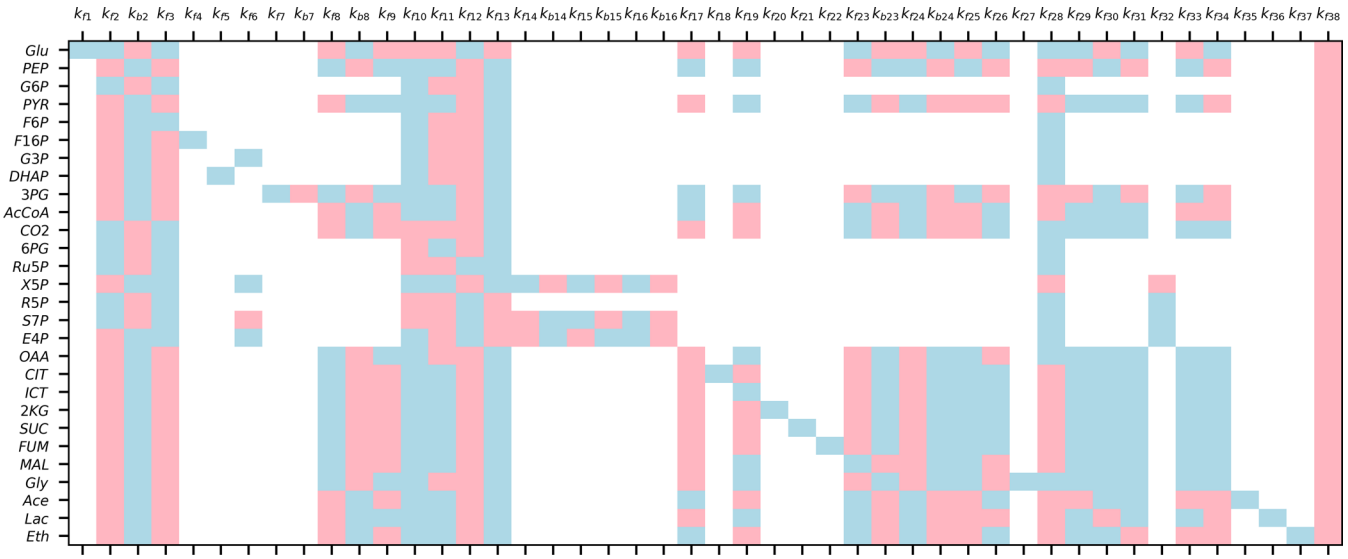

Figure 11. Most probable perturbation response patterns for metabolites in the glycolysis and TCA cycle of *E. coli*. This result is a portion of that shown in Figure 9a. The columns are the rate constants with k_f and k_b for forward and backward reactions, respectively, in the same order as in Figure 8, and the rows are the metabolites.

https://doi.org/10.1021/acsomega.2c06113
ACS Omega 2023, 8, 3043−3056

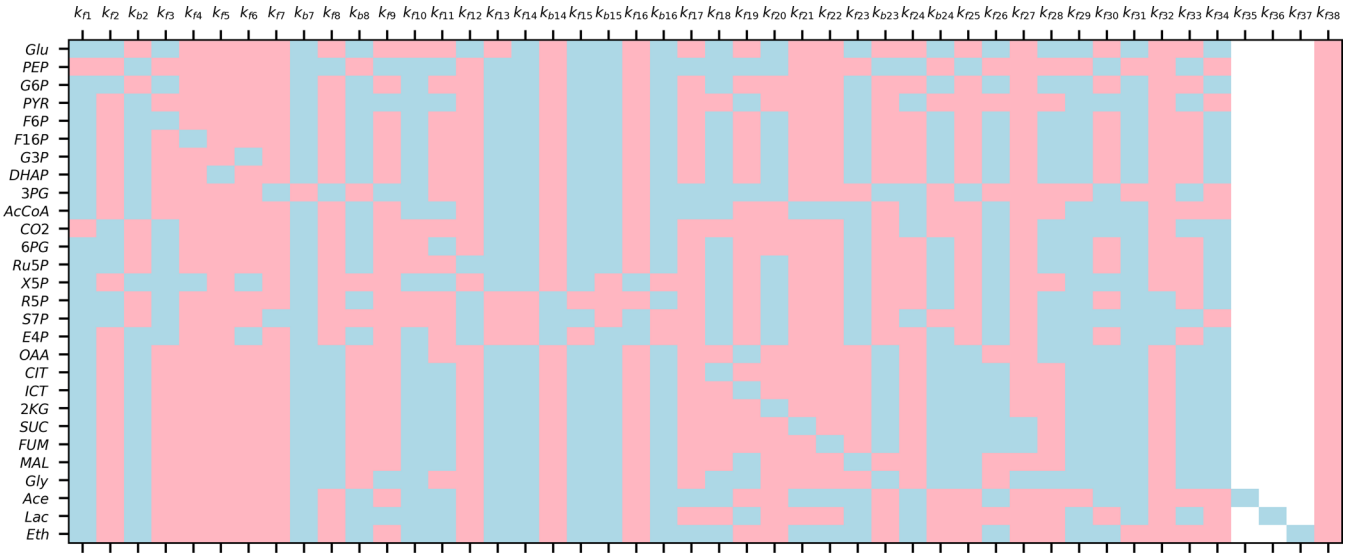

Figure 12. Most probable perturbation response patterns for the variance of the metabolites in the glycolysis and TCA cycle of *E. coli*. This result is a portion of that shown in Figure 9a. The columns are the rate constants with k_f and k_b for forward and backward reactions, respectively, in the same order as in Figure 8, and the rows are the metabolites.

open systems generally show greater uncertainty in the fate of pseudo-components (especially the covariance), subject to perturbation. Nevertheless, our noise localization theory can be useful to discriminate different models compared to experimental data, to help researchers decide how to perturb a given system based on network structure, to render a desired change of state in noise or chemical composition, and to scan interesting noise behavior from a given topological network.

■ ASSOCIATED CONTENT

Supporting Information

The Supporting Information is available free of charge at https://pubs.acs.org/doi/10.1021/acsomega.2c06113.

Steps of noise localization, example of noise localization, and names of species in the carbon metabolic TCA cycle of *E. coli* (PDF)

■ AUTHOR INFORMATION

Corresponding Author

Chao-Ping Hsu − *Institute of Chemistry, Academia Sinica, Taipei 115201, Taiwan; Bioinformatics Program, Institute of Information Science, Taiwan International Graduate Program, Academia Sinica, Taipei 115201, Taiwan; Physics Division, National Center for Theoretical Sciences, Taipei 106319, Taiwan; Genome and Systems Biology Degree Program, National Taiwan University, Taipei 106319, Taiwan;* orcid.org/0000-0002-7187-427X; Email: cherri@chem.sinica.edu.tw

Author

Erickson Fajiculay − *Institute of Chemistry, Academia Sinica, Taipei 115201, Taiwan; Bioinformatics Program, Institute of Information Science, Taiwan International Graduate Program, Academia Sinica, Taipei 115201, Taiwan; Institute of Bioinformatics and Structural Biology, National Tsing Hua University, Hsinchu 300044, Taiwan*

Complete contact information is available at: https://pubs.acs.org/10.1021/acsomega.2c06113

Notes

The authors declare no competing financial interest.

■ ACKNOWLEDGMENTS

The authors gratefully acknowledge support from the National Science and Technology Council (Project 111-2123-M-001-003) and Academia Sinica. They thank Dr. Ching-Cher Sanders Yan and Prof. Je-Chiang Tsai for their helpful discussions.

■ REFERENCES

(1) Elowitz, M. B.; Levine, A. J.; Siggia, E. D.; et al. Stochastic Gene Expression in a Single Cell. *Science* **2002**, *297*, 1183−1186.

(2) Cai, L.; Dalal, C. K.; Elowitz, M. B. Frequency-Modulated Nuclear Localization Bursts Coordinate Gene Regulation. *Nature* **2008**, *455*, 485−490.

(3) Elowitz, M. B.; Leibler, S. A Synthetic Oscillatory Network of Transcriptional Regulators. *Nature* **2000**, *403*, 335−338.

(4) Raj, A.; van Oudenaarden, A. Single-Molecule Approaches to Stochastic Gene Expression. *Annu. Rev. Biophys.* **2009**, *38*, 255−270.

(5) Munsky, B.; Neuert, G.; van Oudenaarden, A. Using Gene Expression Noise to Understand Gene Regulation. *Science* **2012**, *336*, 183−187.

(6) Raj, A.; Rifkin, S. A.; Andersen, E.; van Oudenaarden, A. Variability in Gene Expression Underlies Incomplete Penetrance. *Nature* **2010**, *463*, 913−918.

(7) Vijayan, V.; O'Shea, E. K. Sequence Determinants of Circadian Gene Expression Phase in Cyanobacteria. *J. Bacteriol.* **2013**, *195*, 665−671.

(8) Sutcliffe, E. G.; Bartenbaker Thompson, A.; Stettner, A. R.; Marshall, M. L.; Roberts, M. E.; Susswein, L. R.; Wang, Y.; Klein, R. T.; Hruska, K. S.; Solomon, B. D. Multi-Gene Panel Testing Confirms Phenotypic Variability in MUTYH-Associated Polyposis. *Fam. Cancer* **2019**, *18*, 203−209.

(9) Raser, J. M.; O'Shea, E. K. Noise in Gene Expression: Origins, Consequences, and Control. *Science* **2005**, *309*, 2010−2013.

(10) Raser, J. M.; O'Shea, E. K. Control of Stochasticity in Eukaryotic Gene Expression. *Science* **2004**, *304*, 1811−1814.

(11) Lestas, I.; Vinnicombe, G.; Paulsson, J. Fundamental Limits on the Suppression of Molecular Fluctuations. *Nature* **2010**, *467*, 174−178.

(12) Johnston, I. G.; Gaal, B.; Neves, R. P.; das Enver, T.; Iborra, F. J.; Jones, N. S. Mitochondrial Variability as a Source of Extrinsic Cellular Noise. *PLoS Comput. Biol.* **2012**, *8*, No. e1002416.
(13) Enver, T.; Heyworth, C. M.; Dexter, T. M. Do Stem Cells Play Dice? *Blood* **1998**, *92*, 348−351.
(14) Sardanyés, J.; Alarcón, T. Noise-Induced Bistability in the Fate of Cancer Phenotypic Quasispecies: A Bit-Strings Approach. *Sci. Rep.* **2018**, *8*, No. 1027.
(15) Adnane, S.; Marino, A.; Leucci, E. LncRNAs in Human Cancers: Signal from Noise. *Trends Cell Biol.* **2022**, *32*, 565−573.
(16) Han, R.; Huang, G.; Wang, Y.; Xu, Y.; Hu, Y.; Jiang, W.; Wang, T.; Xiao, T.; Zheng, D. Increased Gene Expression Noise in Human Cancers Is Correlated with Low P53 and Immune Activities as Well as Late Stage Cancer. *Oncotarget* **2016**, *7*, 72011−72020.
(17) Neumeier, D.; Yermanos, A.; Agrafiotis, A.; Csepregi, L.; Chowdhury, T.; Ehling, R. A.; Kuhn, R.; Roberto, R. B.-D.; Di Tacchio, M.; Antonialli, R.; Starkie, D.; Lightwood, D. J.; Oxenius, A.; Reddy, S. T.*Phenotypic Determinism and Stochasticity in Antibody Repertoires of Clonally Expanded Plasma Cells*; bioRxiv, 2021. DOI: 10.1101/2021.07.16.452687.
(18) Carey, J. N.; Mettert, E. L.; Roggiani, M.; Myers, K. S.; Kiley, P. J.; Goulian, M. Regulated Stochasticity in a Bacterial Signaling Network Permits Tolerance to a Rapid Environmental Change. *Cell* **2018**, *173*, 196.e14−207.e14.
(19) Pilpel, Y.Noise in Biological Systems: Pros, Cons, and Mechanisms of Control. In *Yeast Systems Biology: Methods and Protocols*; Castrillo, J. I.; Oliver, S. G., Eds.; Methods in Molecular Biology; Humana Press: Totowa, NJ, 2011; pp 407−425.
(20) Fraser, D.; Kærn, M. A Chance at Survival: Gene Expression Noise and Phenotypic Diversification Strategies. *Mol. Microbiol.* **2009**, *71*, 1333−1340.
(21) Yan, C.-C. S.; Hsu, C.-P. The Fluctuation-Dissipation Theorem for Stochastic Kinetics—Implications on Genetic Regulations. *J. Chem. Phys.* **2013**, *139*, No. 224109.
(22) Johnston, I. The Chaos within: Exploring Noise in Cellular Biology. *Significance* **2012**, *9*, 17−21.
(23) Chang, A. Y.; Marshall, W. F. Organelles − Understanding Noise and Heterogeneity in Cell Biology at an Intermediate Scale. *J. Cell Sci.* **2017**, 819.
(24) Stoeger, T.; Battich, N.; Pelkmans, L. Passive Noise Filtering by Cellular Compartmentalization. *Cell* **2016**, *164*, 1151−1161.
(25) Sun, X.; Zhang, J.; Zhao, Q.; Chen, X.; Zhu, W.; Yan, G.; Zhou, T. Stochastic Modeling Suggests That Noise Reduces Differentiation Efficiency by Inducing a Heterogeneous Drug Response in Glioma Differentiation Therapy. *BMC Syst. Biol.* **2016**, *10*, No. 73.
(26) Bersani, A. M.; Bersani, E.; Mastroeni, L. Deterministic and Stochastic Models of Enzymatic Networks—Applications to Pharmaceutical Research. *Comput. Math. Appl.* **2008**, *55*, 879−888.
(27) Dar, R. D.; Hosmane, N. N.; Arkin, M. R.; Siliciano, R. F.; Weinberger, L. S. Screening for Noise in Gene Expression Identifies Drug Synergies. *Science* **2014**, *344*, 1392−1396.
(28) Gillespie, D. T. Stochastic Simulation of Chemical Kinetics. *Annu. Rev. Phys. Chem.* **2007**, *58*, 35−55.
(29) Gillespie, D. T. A Rigorous Derivation of the Chemical Master Equation. *Phys. A* **1992**, *188*, 404−425.
(30) Gillespie, D. T. Exact Stochastic Simulation of Coupled Chemical Reactions. *J. Phys. Chem. A* **1977**, *81*, 2340−2361.
(31) Cao, Y.; Gillespie, D. T.; Petzold, L. R. Efficient Step Size Selection for the Tau-Leaping Simulation Method. *J. Chem. Phys.* **2006**, *124*, No. 044109.
(32) Wu, S.; Fu, J.; Petzold, L. R. Adaptive Deployment of Model Reductions for Tau-Leaping Simulation. *J. Chem. Phys.* **2015**, *142*, No. 204108.
(33) Gillespie, D. T. The Chemical Langevin Equation. *J. Chem. Phys.* **2000**, *113*, 297−306.
(34) Han, X.; Valorani, M.; Najm, H. N. Explicit Time Integration of the Stiff Chemical Langevin Equations Using Computational Singular Perturbation. *J. Chem. Phys.* **2019**, *150*, No. 194101.
(35) Wu, F.; Tian, T.; Rawlings, J. B.; Yin, G. Approximate Method for Stochastic Chemical Kinetics with Two-Time Scales by Chemical Langevin Equations. *J. Chem. Phys.* **2016**, *144*, No. 174112.
(36) Ceccato, A.; Frezzato, D. Remarks on the Chemical Fokker-Planck and Langevin Equations: Nonphysical Currents at Equilibrium. *J. Chem. Phys.* **2018**, *148*, No. 064114.
(37) Sotiropoulos, V.; Contou-Carrere, M.-N.; Daoutidis, P.; Kaznessis, Y. N. Model Reduction of Multiscale Chemical Langevin Equations: A Numerical Case Study. *IEEE/ACM Trans. Comput. Biol. Bioinf.* **2009**, *6*, 470−482.
(38) Bishwal, J. P. N. In *Parameter Estimation in Stochastic Differential Equations*; Morel, J.-M.; Takens, F.; Teissier, B., Eds.; Lecture Notes in Mathematics; Springer: Berlin, Heidelberg, 2008; Vol. *1923*.
(39) Liu, Y.; Gunawan, R. Parameter Estimation of Dynamic Biological Network Models Using Integrated Fluxes. *BMC Syst. Biol.* **2014**, *8*, No. 127.
(40) Mitra, E. D.; Hlavacek, W. S. Parameter Estimation and Uncertainty Quantification for Systems Biology Models. *Curr. Opin. Syst. Biol.* **2019**, *18*, 9−18.
(41) Abdulla, U. G.; Poteau, R. Identification of Parameters in Systems Biology. *Math. Biosci.* **2018**, *305*, 133−145.
(42) Pullen, N.; Morris, R. J. Bayesian Model Comparison and Parameter Inference in Systems Biology Using Nested Sampling. *PLoS One* **2014**, *9*, No. e88419.
(43) Browning, A. P.; Warne, D. J.; Burrage, K.; Baker, R. E.; Simpson, M. J. Identifiability Analysis for Stochastic Differential Equation Models in Systems Biology. *J. R. Soc., Interface* **2020**, *17*, No. 20200652.
(44) Saccomani, M. P.Identifiability of Nonlinear ODE Models in Systems Biology: Results from Both Structural and Data-Based Methods. In *Bioinformatics and Biomedical Engineering*; Ortuño, F.; Rojas, I., Eds.; Springer International Publishing: Cham, 2015; pp 650−658.
(45) Chis, O.-T.; Banga, J. R.; Balsa-Canto, E. Structural Identifiability of Systems Biology Models: A Critical Comparison of Methods. *PLoS One* **2011**, *6*, No. e27755.
(46) Dobre, S.; Bastogne, T.; Richard, A. Global Sensitivity and Identifiability Implications in Systems Biology. *IFAC Proc. Vol.* **2010**, *43*, 54−59.
(47) von Dassow, G.; Meir, E.; Munro, E. M.; Odell, G. M. The Segment Polarity Network Is a Robust Developmental Module. *Nature* **2000**, *406*, 188−192.
(48) Eldar, A.; Dorfman, R.; Weiss, D.; Ashe, H.; Shilo, B.-Z.; Barkai, N. Robustness of the BMP Morphogen Gradient in Drosophila Embryonic Patterning. *Nature* **2002**, *419*, 304−308.
(49) Meir, E.; von Dassow, G.; Munro, E.; Odell, G. M. Robustness, Flexibility, and the Role of Lateral Inhibition in the Neurogenic Network. *Curr. Biol.* **2002**, *12*, 778−786.
(50) Joanito, I.; Yan, C.-C. S.; Chu, J.-W.; Wu, S.-H.; Hsu, C.-P. Basal Leakage in Oscillation: Coupled Transcriptional and Translational Control Using Feed-Forward Loops. *PLoS Comput. Biol.* **2020**, *16*, No. e1007740.
(51) Sumner, T.; Shephard, E.; Bogle, I. D. L. A Methodology for Global-Sensitivity Analysis of Time-Dependent Outputs in Systems Biology Modelling. *J. R. Soc., Interface* **2012**, *9*, 2156−2166.
(52) Hsu, C.-P.; Lee, P.-H.; Chang, C.-W.; Lee, C.-T. Constructing Quantitative Models from Qualitative Mutant Phenotypes: Preferences in Selecting Sensory Organ Precursors. *Bioinformatics* **2006**, *22*, 1375−1382.
(53) Joanito, I.; Chu, J.-W.; Wu, S.-H.; Hsu, C.-P. An Incoherent Feed-Forward Loop Switches the Arabidopsis Clock Rapidly between Two Hysteretic States. *Sci. Rep.* **2018**, *8*, No. 13944.
(54) Elf, J.; Ehrenberg, M. Fast Evaluation of Fluctuations in Biochemical Networks With the Linear Noise Approximation. *Genome Res.* **2003**, *13*, 2475−2484.
(55) While the term "noise" is often referred as the coefficient of variation, defined as the standard deviation divided by the mean of a stochastic quantity, here, following the linear noise approximation literature, and for the sake of conciseness and readability, through out the text the term "noise" is broadly used for variance and covariances.

https://doi.org/10.1021/acsomega.2c06113
ACS Omega 2023, 8, 3043−3056

(56) Fajiculay, E.; Hsu, C.-P. BioSANS: A Software Package for Symbolic and Numeric Biological Simulation. *PLoS One* **2022**, *17*, No. e0256409.
(57) Paulsson, J. Summing up the Noise in Gene Networks. *Nature* **2004**, *427*, 415−418.
(58) Hayot, F.; Jayaprakash, C. The Linear Noise Approximation for Molecular Fluctuations within Cells. *Phys. Biol.* **2004**, *1*, 205−210.
(59) Lötstedt, P. The Linear Noise Approximation for Spatially Dependent Biochemical Networks. *Bull. Math. Biol.* **2019**, *81*, 2873−2901.
(60) Wu, H.-W.; Fajiculay, E.; Wu, J.-F.; Yan, C.-C. S.; Hsu, C.-P.; Wu, S.-H. Noise Reduction by Upstream Open Reading Frames. *Nat. Plants* **2022**, *8*, 474−480.
(61) Komorowski, M.; Miękisz, J.; Stumpf, M. P. H. Decomposing Noise in Biochemical Signaling Systems Highlights the Role of Protein Degradation. *Biophys. J.* **2013**, *104*, 1783−1793.
(62) Okada, T.; Mochizuki, A. Law of Localization in Chemical Reaction Networks. *Phys. Rev. Lett.* **2016**, *117*, No. 048101.
(63) Mochizuki, A.; Fiedler, B. Sensitivity of Chemical Reaction Networks: A Structural Approach. 1. Examples and the Carbon Metabolic Network. *J. Theor. Biol.* **2015**, *367*, 189−202.
(64) Ishii, N.; Nakahigashi, K.; Baba, T.; Robert, M.; Soga, T.; Kanai, A.; Hirasawa, T.; Naba, M.; Hirai, K.; Hoque, A.; Ho, P. Y.; Kakazu, Y.; Sugawara, K.; Igarashi, S.; Harada, S.; Masuda, T.; Sugiyama, N.; Togashi, T.; Hasegawa, M.; Takai, Y.; Yugi, K.; Arakawa, K.; Iwata, N.; Toya, Y.; Nakayama, Y.; Nishioka, T.; Shimizu, K.; Mori, H.; Tomita, M. Multiple High-Throughput Analyses Monitor the Response of *E. coli* to Perturbations. *Science* **2007**, *316*, 593−597.
(65) Ni, X. Y.; Drengstig, T.; Ruoff, P. The Control of the Controller: Molecular Mechanisms for Robust Perfect Adaptation and Temperature Compensation. *Biophys. J.* **2009**, *97*, 1244−1253.
(66) Okada, T.; Tsai, J.-C.; Mochizuki, A. Structural Bifurcation Analysis in Chemical Reaction Networks. *Phys. Rev. E* **2018**, *98*, No. 012417.
(67) Okada, T.; Mochizuki, A.; Furuta, M.; Tsai, J.-C. Flux-Augmented Bifurcation Analysis in Chemical Reaction Network Systems. *Phys. Rev. E* **2021**, *103*, No. 062212.
(68) Feng, C.; Song, C.; Liu, Y.; Qian, F.; Gao, Y.; Ning, Z.; Wang, Q.; Jiang, Y.; Li, Y.; Li, M.; Chen, J.; Zhang, J.; Li, C. KnockTF: A Comprehensive Human Gene Expression Profile Database with Knockdown/Knockout of Transcription Factors. *Nucleic Acids Res.* **2020**, *48*, D93−D100.
(69) Keenan, A. B.; Jenkins, S. L.; Jagodnik, K. M.; Koplev, S.; He, E.; Torre, D.; Wang, Z.; Dohlman, A. B.; Silverstein, M. C.; Lachmann, A.; Kuleshov, M. V.; Ma'ayan, A.; Stathias, V.; Terryn, R.; Cooper, D.; Forlin, M.; Koleti, A.; Vidovic, D.; Chung, C.; Schürer, S. C.; Vasiliauskas, J.; Pilarczyk, M.; Shamsaei, B.; Fazel, M.; Ren, Y.; Niu, W.; Clark, N. A.; White, S.; Mahi, N.; Zhang, L.; Kouril, M.; Reichard, J. F.; Sivaganesan, S.; Medvedovic, M.; Meller, J.; Koch, R. J.; Birtwistle, M. R.; Iyengar, R.; Sobie, E. A.; Azeloglu, E. U.; Kaye, J.; Osterloh, J.; Haston, K.; Kalra, J.; Finkbiener, S.; Li, J.; Milani, P.; Adam, M.; Escalante-Chong, R.; Sachs, K.; Lenail, A.; Ramamoorthy, D.; Fraenkel, E.; Daigle, G.; Hussain, U.; Coye, A.; Rothstein, J.; Sareen, D.; Ornelas, L.; Banuelos, M.; Mandefro, B.; Ho, R.; Svendsen, C. N.; Lim, R. G.; Stocksdale, J.; Casale, M. S.; Thompson, T. G.; Wu, J.; Thompson, L. M.; Dardov, V.; Venkatraman, V.; Matlock, A.; Van Eyk, J. E.; Jaffe, J. D.; Papanastasiou, M.; Subramanian, A.; Golub, T. R.; Erickson, S. D.; Fallahi-Sichani, M.; Hafner, M.; Gray, N. S.; Lin, J.-R.; Mills, C. E.; Muhlich, J. L.; Niepel, M.; Shamu, C. E.; Williams, E. H.; Wrobel, D.; Sorger, P. K.; Heiser, L. M.; Gray, J. W.; Korkola, J. E.; Mills, G. B.; LaBarge, M.; Feiler, H. S.; Dane, M. A.; Bucher, E.; Nederlof, M.; Sudar, D.; Gross, S.; Kilburn, D. F.; Smith, R.; Devlin, K.; Margolis, R.; Derr, L.; Lee, A.; Pillai, A. The Library of Integrated Network-Based Cellular Signatures NIH Program: System-Level Cataloging of Human Cells Response to Perturbations. *Cell Syst.* **2018**, *6*, 13−24.
(70) Cho, Y. J.; Ramakrishnan, N.; Cao, Y. In *Reconstructing Chemical Reaction Networks: Data Mining Meets System Identification*, Proceeding of the 14th ACM SIGKDD International Conference on Knowledge Discovery and Data Mining—KDD 08 2008; pp 1−9.
(71) Choon, W. Y.; Mohamad, M. S.Reconstructing Metabolic Networks − A Review. *Advances in Bioinformatics: Reviews and Applications*; UTM Press, 2011; Vol. *16*.
(72) Zheng, X.; Huang, Y.; Zou, X. ScPADGRN: A Preconditioned ADMM Approach for Reconstructing Dynamic Gene Regulatory Network Using Single-Cell RNA Sequencing Data. *PLoS Comput. Biol.* **2020**, No. e1007471.
(73) Liu, Z.-P. Towards Precise Reconstruction of Gene Regulatory Networks by Data Integration. *Quant. Biol.* **2018**, *6*, 113−128.
(74) Zheng, G.; Huang, T.The Reconstruction and Analysis of Gene Regulatory Networks. In *Computational Systems Biology: Methods and Protocols*; Huang, T., Ed.; Methods in Molecular Biology; Humana Press: New York, NY, 2018; pp 137−154.
(75) Ward, C.; Yeung, E.; Brown, T.; Durtschi, B.; Weyerman, S.; Howes, R.; Goncalves, J.; Warnick, S.*A Comparison of Network Reconstruction Methods for Chemical Reaction Networks*, The Proceedings of the Third International Conference on Foundations of Systems Biology in Engineering (FOSBE 2009), 2009.
(76) Baumler, D. J.; Peplinski, R. G.; Reed, J. L.; Glasner, J. D.; Perna, N. T. The Evolution of Metabolic Networks of *E. coli*. *BMC Syst. Biol.* **2011**, *5*, No. 182.
(77) Payne, D. D.; Renz, A.; Dunphy, L. J.; Lewis, T.; Dräger, A.; Papin, J. A. An Updated Genome-Scale Metabolic Network Reconstruction of Pseudomonas Aeruginosa PA14 to Characterize Mucin-Driven Shifts in Bacterial Metabolism. *npj Syst. Biol. Appl.* **2021**, *7*, No. 37.
(78) Donckels, B. M. R.Optimal Experimental Design, Model Discrimination. In *Encyclopedia of Systems Biology*; Dubitzky, W.; Wolkenhauer, O.; Cho, K.-H.; Yokota, H., Eds.; Springer: New York, NY, 2013; pp 1593−1596.
(79) Gunawardena, J. Models in Biology: 'Accurate Descriptions of Our Pathetic Thinking'. *BMC Biol.* **2014**, *12*, No. 29.
(80) Gupta, U.; Le, T.; Hu, W.-S.; Bhan, A.; Daoutidis, P. Automated Network Generation and Analysis of Biochemical Reaction Pathways Using RING. *Metab. Eng.* **2018**, *49*, 84−93.
(81) Jahnke, T.; Huisinga, W. Solving the Chemical Master Equation for Monomolecular Reaction Systems Analytically. *J. Math. Biol.* **2006**, *54*, 1−26.
(82) Kampen, N. G. V.*Stochastic Processes in Physics and Chemistry*, 3rd ed.; North Holland: Amsterdam, 2007.
(83) Risken, H.Fokker-Planck Equation. In *The Fokker-Planck Equation: Methods of Solution and Applications*; Risken, H., Ed.; Springer Series in Synergetics; Springer: Berlin, Heidelberg, 1996; pp 63−95.
(84) Parks, P. C. A. M. Lyapunov's Stability Theory—100 Years On. *IMA J. Math. Control Inf.* **1992**, *9*, 275−303.
(85) Ishii, N.; Nakahigashi, K.; Baba, T.; Robert, M.; Soga, T.; Kanai, A.; Hirasawa, T.; Naba, M.; Hirai, K.; Hoque, A.; Ho, P. Y.; Kakazu, Y.; Sugawara, K.; Igarashi, S.; Harada, S.; Masuda, T.; Sugiyama, N.; Togashi, T.; Hasegawa, M.; Takai, Y.; Yugi, K.; Arakawa, K.; Iwata, N.; Toya, Y.; Nakayama, Y.; Nishioka, T.; Shimizu, K.; Mori, H.; Tomita, M. Multiple High-Throughput Analyses Monitor the Response of *E. coli* to Perturbations. *Science* **2007**, *316*, 593−597.
(86) Wishart, D. S.; Tzur, D.; Knox, C.; Eisner, R.; Guo, A. C.; Young, N.; Cheng, D.; Jewell, K.; Arndt, D.; Sawhney, S.; Fung, C.; Nikolai, L.; Lewis, M.; Coutouly, M.-A.; Forsythe, I.; Tang, P.; Shrivastava, S.; Jeroncic, K.; Stothard, P.; Amegbey, G.; Block, D.; Hau; David, D.; Wagner, J.; Miniaci, J.; Clements, M.; Gebremedhin, M.; Guo, N.; Zhang, Y.; Duggan, G. E.; MacInnis, G. D.; Weljie, A. M.; Dowlatabadi, R.; Bamforth, F.; Clive, D.; Greiner, R.; Li, L.; Marrie, T.; Sykes, B. D.; Vogel, H. J.; Querengesser, L. HMDB: The Human Metabolome Database. *Nucleic Acids Res.* **2007**, *35*, D521−D526.

https://doi.org/10.1021/acsomega.2c06113
ACS Omega 2023, 8, 3043−3056